

Study on the Reduction Behavior of Zirconia Supported Iron Oxide Catalysts by Temperature-Programmed Reduction Combined with *in Situ* Mössbauer Spectroscopy

Kaidong Chen, Yining Fan, Zheng Hu, and Qijie Yan¹

Department of Chemistry, Nanjing University, Nanjing 210093, China

Received May 1, 1995; in revised form September 21, 1995; accepted September 22, 1995

The reduction properties of Fe₂O₃/ZrO₂ catalysts with various Fe₂O₃ loading and the interactions between iron oxide and zirconia have been studied by using temperature-programmed reduction combined with *in situ* Mössbauer spectroscopy. This is shown that the intermediates formed during reduction depend strongly not only on the reduction temperature but also on the iron loading. Several iron species such as bulk phase α -Fe₂O₃, small α -Fe₂O₃ particles, and surface iron oxide species are found in the zirconia supported iron oxide catalysts. Reduction of the small α -Fe₂O₃ particles is easier than that of the bulk phase α -Fe₂O₃. In contrast, the surface iron oxide species are much more difficult to reduce because of their strong interactions with the support. The phenomena of partial oxidation of Fe²⁺ cations and Fe₃O₄ to Fe³⁺ cations in the reduction processes are observed. © 1996 Academic Press, Inc.

INTRODUCTION

The interactions between metal oxide and support have gained growing interest in the past two decades, much attention has been given to the study of the reduction properties of supported metal oxide catalysts. Among these, supported iron oxide catalysts are of particular importance because of their extensive applications in many catalytic processes (1, 2). Tang Ren-Yuan *et al.* (3) were the first to use an *in situ* combined temperature-programmed reduction–Mössbauer spectroscopic technique to study the reduction of alumina supported iron catalysts, and they confirmed that the technique is very effective in studying the reduction process and intermediates of supported iron catalysts. Lund *et al.* (4–7) reported that the activity of magnetite particles for the water–gas shift reaction was greatly depressed when the particles were supported on silica. By using NO chemisorption and Mössbauer spectroscopy, they found that by substituting for Si⁴⁺ cations from the support, the Fe³⁺ cations in the surface tetrahedral

sites of the magnetite could migrate to adjacent octahedral sites. XingTao Gao *et al.* (8) studied the reduction properties of Fe₂O₃/TiO₂ and Fe₂O₃/Al₂O₃ systems. They found that the properties of the support play an important role in determining the reduction intermediates of supported iron oxides, due to the different interactions between iron oxide and the supports. Different surface species can be formed by the interactions between metal oxide and various supports (9, 10), which in turn will affect the surface states and related properties of the catalysts.

Besides the nature of the support, the preparation conditions, especially the loading of metal oxide and calcination temperature and duration, can have a strong impact on the nature of the interactions between metal oxides and supports (11–14), hence influence the reduction behavior of the sample. For example, in a silica supported iron oxide sample with a loading of 1 wt% Fe, the high-coordination Fe²⁺ cations can be converted into low-coordination Fe²⁺ cations under severe reduction conditions (10). In another study, Fe³⁺ cations were found to transfer from octahedral to tetrahedral sites when the Fe₂O₃/SiO₂ sample was treated in oxygen at 773 K for 16 hr (13).

Zirconia is currently attracting considerable scientific interest for its potential use as a catalyst support or promoter for a variety of catalyst systems (15). F. J. Berry *et al.* (16) prepared iron–zirconia catalysts by the coprecipitation method and studied their catalytic properties for hydrogenation of CO. In our recent work, we also found that Fe₂O₃/ZrO₂ catalysts prepared by the impregnation method could markedly suppress the formation of methane when they were used in CO hydrogenation. The aim of this work is to study the reduction properties of Fe₂O₃/ZrO₂ catalysts with various iron oxide loading and the interactions between iron oxide and zirconia.

Temperature-programmed reduction combined with *in situ* Mössbauer spectroscopy is used in this work to study the formation of various intermediates during the successive steps of reduction of iron oxide deposited on zirconia. Along these lines, the interactions between iron oxide and zirconia is discussed.

¹ To whom correspondence should be addressed.

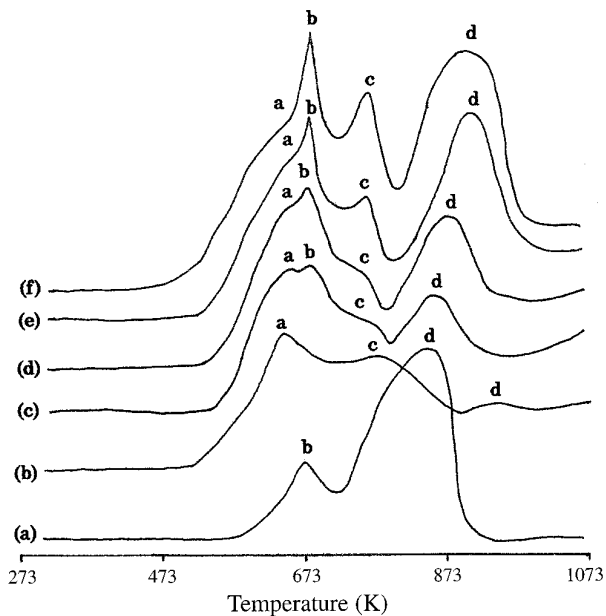


FIG. 1. TPR profiles of $\text{Fe}_2\text{O}_3/\text{ZrO}_2$ catalysts with various Fe_2O_3 loading. (a) Bulk $\alpha\text{-Fe}_2\text{O}_3$, (b) 1.6 wt%, (c) 3 wt%, (d) 4 wt%, (e) 5 wt%, and (f) 7 wt%.

EXPERIMENTAL

$\text{Fe}_2\text{O}_3/\text{ZrO}_2$ catalysts with various Fe_2O_3 loading were prepared by impregnating zirconia (surface area $39 \text{ m}^2/\text{g}$, C. P. Shanghai) with an aqueous solution of iron nitrate, and then dried at 393 K and calcined at 773 K for 5 hr. X-ray diffraction measurements were performed on a Rigaku D/max-rA diffractometer using $\text{CuK}\alpha$ radiation. The TPR experiments were carried out in a U-type quartz reactor with a heating rate of $16 \text{ K}/\text{min}$ and a flow rate of $\text{H}_2\text{-Ar}$

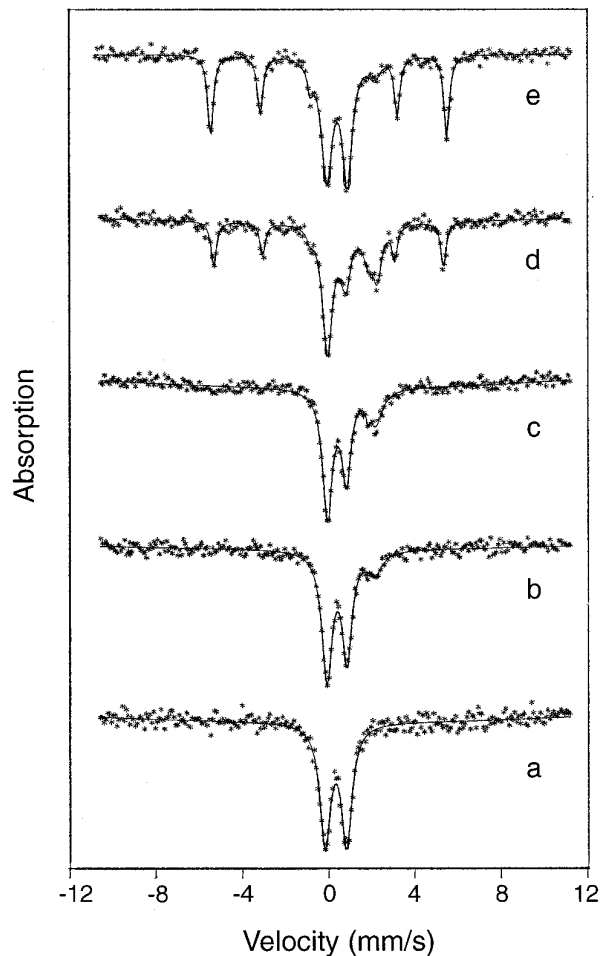


FIG. 2. Mössbauer spectra of 1.6 wt% $\text{Fe}_2\text{O}_3/\text{ZrO}_2$ catalyst treated at various conditions. (a) As-prepared, (b) TPR to 643 K , (c) TPR to 753 K , (d) TPR to 973 K , (e) TPR to 1073 K .

TABLE 1
Mössbauer Parameters of 1.6 wt% $\text{Fe}_2\text{O}_3/\text{ZrO}_2$ Catalyst Treated under Various Conditions

| Treatment condition | Mössbauer parameter | | | Iron species | Relative area (%) |
|-------------------------|---------------------|-------------|-----------|------------------|-------------------|
| | IS (mm/sec) | QS (mm/sec) | H (KOe) | | |
| As-prepared | 0.38 | 1.01 | 0 | Fe^{3+} | 100 |
| TPR to 643 K | 0.39 | 0.94 | 0 | Fe^{3+} | 76 |
| | 1.03 | 2.23 | 0 | Fe^{2+} | 24 |
| TPR to 753 K | 0.38 | 0.92 | 0 | Fe^{3+} | 61 |
| | 1.06 | 2.14 | 0 | Fe^{2+} | 39 |
| TPR to 973 K | 0.04 | 0.00 | 331 | Fe^0 | 26 |
| | 0.37 | 0.89 | 0 | Fe^{3+} | 31 |
| | 1.08 | 2.25 | 0 | Fe^{2+} | 43 |
| TPR to 1073 K | 0.01 | 0.00 | 338 | Fe^0 | 41 |
| | 0.38 | 0.93 | 0 | Fe^{3+} | 50 |
| | 0.99 | 2.24 | 0 | Fe^{2+} | 9 |

TABLE 2
Mössbauer Parameters of 7 wt% Fe₂O₃/ZrO₂ Catalyst Treated under Various Conditions

| Treatment condition | Mössbauer parameter | | | Iron species | Relative area (%) |
|---------------------|---------------------|-------------|---------|-------------------------------------|-------------------|
| | IS (mm/sec) | QS (mm/sec) | H (KOe) | | |
| As-prepared | 0.43 | -0.12 | 511 | Fe ³⁺ | 53 |
| | 0.35 | 1.03 | 0 | Fe ³⁺ | 47 |
| TPR to 673 K | 0.32 | -0.07 | 490 | Fe ³⁺ | 13 |
| | 0.77 | 0.00 | 467 | Fe ³⁺ , Fe ²⁺ | 40 |
| | 0.38 | 1.04 | 0 | Fe ³⁺ | 47 |
| TPR to 753 K | 1.06 | 0.00 | 0 | Fe ²⁺ | 38 |
| | 0.46 | 1.01 | 0 | Fe ³⁺ | 62 |
| TPR to 973 K | 0.02 | 0.02 | 334 | Fe ⁰ | 72 |
| | 0.38 | 0.99 | 0 | Fe ³⁺ | 28 |
| TPR to 1073 K | 0.00 | 0.01 | 338 | Fe ⁰ | 83 |
| | 0.42 | 0.99 | 0 | Fe ³⁺ | 17 |

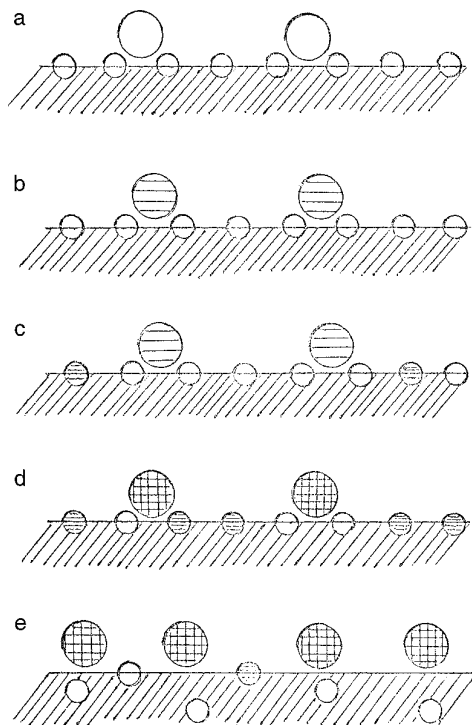


FIG. 3. Pictorial models for the reduction of the 1.6 wt% Fe₂O₃/ZrO₂ catalyst. (a) As-prepared, (b) TPR to 643 K, (c) TPR to 753 K, (d) TPR to 973 K, (e) TPR to 1073 K. ○ Fe³⁺ cations from the surface iron oxides; ○ Small Fe₂O₃ particles; ⊕ Fe²⁺ cations from the reduction of the surface Fe³⁺ cations; ⊕ FeO from the reduction of the small Fe₂O₃ particles; ● Metallic iron particles; ▨ Surface of the zirconia support.

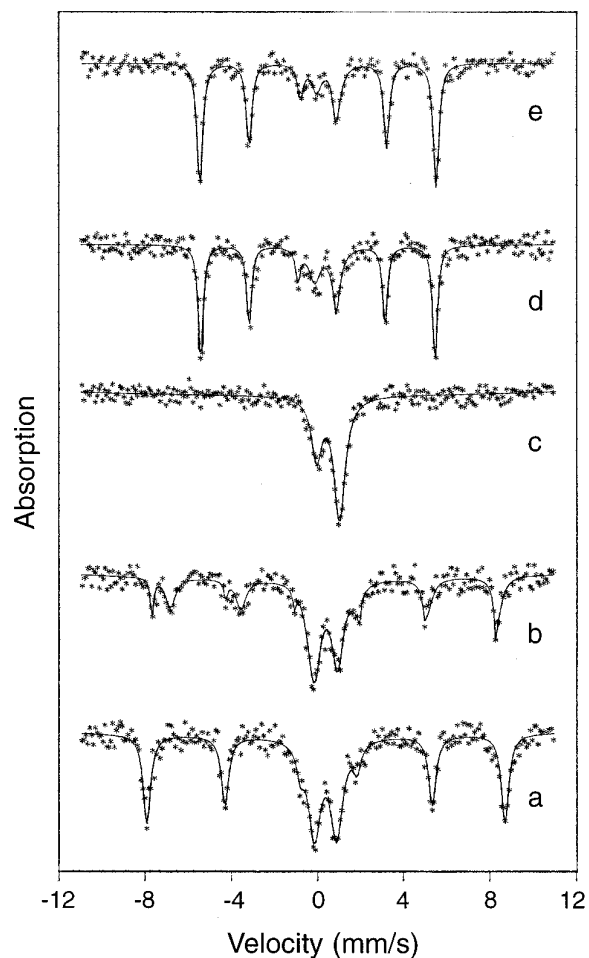


FIG. 4. Mössbauer spectra of 7 wt% Fe₂O₃/ZrO₂ catalyst treated at various conditions. (a) As-prepared, (b) TPR to 673 K, (c) TPR to 753 K, (d) TPR to 973 K, (e) TPR to 1073 K.

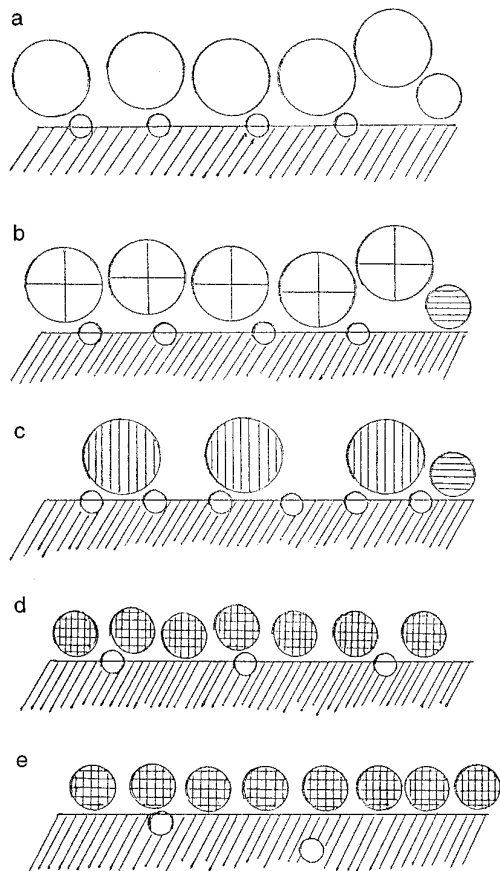


FIG. 5. Pictorial models for the reduction of the 7 wt% $\text{Fe}_2\text{O}_3/\text{ZrO}_2$ catalyst. (a) As-prepared, (b) TPR to 673 K, (c) TPR to 753 K, (d) TPR to 973 K, (e) TPR to 1073 K. \circ Fe^{3+} cations from the surface iron oxides; \circ Small Fe_2O_3 particles; \bigcirc Bulk phase Fe_2O_3 particles; \ominus Fe^{2+} cations from the reduction of the surface Fe^{3+} cations; \ominus FeO from the reduction of the small Fe_2O_3 particles; \ominus FeO from the reduction of the Fe_3O_4 particles; \oplus Fe_3O_4 particles; \bullet Metallic iron particles; ||||| Surface of the zirconia support.

mixture (5.0 vol% hydrogen) ca. 30 ml/min. Hydrogen consumption was monitored by a thermal conductivity detector. Before each TPR run, the as-prepared sample was heated *in situ* with dry air at 393 K for 1 hr. Mössbauer spectroscopy experiments were conducted with a constant acceleration spectrometer using a 10 mCi $^{57}\text{Co}/\text{Pd}$ source. All spectra were computer fitted to a Lorentzian line shape with a least-squares fitting procedure, and the isomer shifts (IS) were given with respect to the centroid of $\alpha\text{-Fe}$ at room temperature. For the Mössbauer tests of the samples with iron oxide loading less than 4 wt%, ^{57}Fe enriched iron containing 83% ^{57}Fe was used.

The experimental procedure for the combined *in situ* TPR–Mössbauer spectroscopy was as follows. First, a TPR run was performed to a temperature as high as possible to obtain an integrated reduction profile. According to the integrated profile, new TPR runs were carried out to a

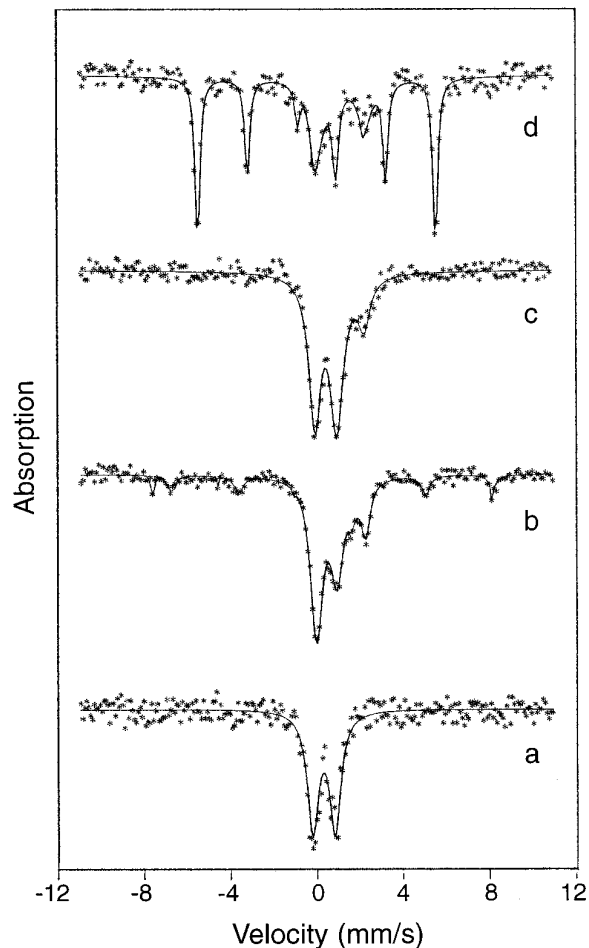


FIG. 6. Mössbauer spectra of 4 wt% $\text{Fe}_2\text{O}_3/\text{ZrO}_2$ catalyst treated at various conditions. (a) As-prepared, (b) TPR to 673 K, (c) TPR to 753 K, (d) TPR to 973 K.

given temperature corresponding to different reduction stages and held for several minutes to allow for the hydrogen consumption of the whole peak. Then the sample was cooled under an argon–hydrogen flow to room temperature and transferred into the Mössbauer cell under the protection of nitrogen for the corresponding Mössbauer measurement. A fresh sample with the same amount was used for each of the runs.

RESULTS AND DISCUSSION

TPR

TPR profiles of the $\text{Fe}_2\text{O}_3/\text{ZrO}_2$ catalysts are shown in Fig. 1. For unsupported bulk $\alpha\text{-Fe}_2\text{O}_3$, two peaks corresponding to the reduction of $\alpha\text{-Fe}_2\text{O}_3$ to Fe_3O_4 and of Fe_3O_4 to $\alpha\text{-Fe}$, respectively (17), are observed. For the $\text{Fe}_2\text{O}_3/\text{ZrO}_2$ catalysts, the TPR profiles are quite different from that of the unsupported $\alpha\text{-Fe}_2\text{O}_3$ and change with the loading of iron oxide. Apparently, the interactions between

iron oxide and zirconia lead to the formation of different iron-containing species with different reducibilities. When the amount of iron oxide was increased, the relative area of peak (a) at ca. 643 K decreased while those of peak (b), (c), and (d) at ca. 673, 753, and 903 K, respectively, increased. It is reasonable to consider that the supported Fe^{3+} species might exist in the following different states: (i) large particles or bulk phase $\alpha\text{-Fe}_2\text{O}_3$ (X-ray diffraction lines for $\alpha\text{-Fe}_2\text{O}_3$ can be observed in the XRD pattern), (ii) small $\alpha\text{-Fe}_2\text{O}_3$ particles, and (iii) surface species formed by the strong interactions of iron oxide and zirconia. If there were no interactions between Fe^{3+} species and the support, the small $\alpha\text{-Fe}_2\text{O}_3$ particles should be more easily reduced than the bulk phase $\alpha\text{-Fe}_2\text{O}_3$ (18). Compared to the reduction profile of unsupported $\alpha\text{-Fe}_2\text{O}_3$, peak (b) with a maximum at 673 K can be assigned to the reduction of bulk $\alpha\text{-Fe}_2\text{O}_3$ to Fe_3O_4 . Peak (a) may originate from the reduction of small $\alpha\text{-Fe}_2\text{O}_3$ particles which have very weak interactions with the support. Peak (c) may correspond to the reduction of the surface iron oxide species and/or the intermediates formed in the first (peak a) and the second (peak b) reduction steps. During the fourth reduction stage with peak (d), iron oxides are reduced to $\alpha\text{-Fe}$. This assignment is consistent with the result that the relative area of peak (b), (c), and (d) increases while that of peak (a) decreases with increasing iron oxide loading, since the increase of iron oxide loading would lead to the increase of large $\alpha\text{-Fe}_2\text{O}_3$ particles.

Reduction of the Low Loading (1.6 wt% Fe_2O_3) $\text{Fe}_2\text{O}_3/\text{ZrO}_2$ Catalyst

The room-temperature Mössbauer spectra of the 1.6 wt% $\text{Fe}_2\text{O}_3/\text{ZrO}_2$ sample reduced at 643, 753, 973, and 1073 K, respectively, are shown in Fig. 2. The spectrum of

the as-prepared sample can be fitted by a doublet with parameters typical of superparamagnetic Fe^{3+} cations (19). In the TPR profile of this sample, peak (b) which corresponds to the reduction of the bulk phase $\alpha\text{-Fe}_2\text{O}_3$ does not appear, indicating that no large $\alpha\text{-Fe}_2\text{O}_3$ particles exist in the sample. After the sample is reduced at 643 K, Mössbauer results (Table 1) reveal that 24% Fe^{3+} cations are reduced to Fe^{2+} cations, while most of the Fe^{3+} cations are not reduced due to the strong interaction with zirconia. Based on the above TPR and Mössbauer spectroscopic results, one can assume that there are two kinds of Fe^{3+} cations in the sample: (i) small $\alpha\text{-Fe}_2\text{O}_3$ particles which have very weak interactions with the support and are easier to reduce than the bulk phase $\alpha\text{-Fe}_2\text{O}_3$, and (ii) surface iron oxide species which have strong interactions with the support and are difficult to reduce. From Table 1 it can be seen that along with the increase in the reduction temperature from 643 to 973 K, more and more Fe^{3+} cations are reduced. After the sample is treated at 973 K, 26% Fe^{2+} cations which are thought to originate from the reduction of the small $\alpha\text{-Fe}_2\text{O}_3$ particles are reduced to $\alpha\text{-Fe}$. In contrast, the Fe^{2+} cations originating from the surface iron oxide species are not reduced due to their strong interactions with the support.

Further increase of the reduction temperature from 973 to 1073 K leads to a dramatic alternation of the catalyst. Along with the reduction of Fe^{2+} to $\alpha\text{-Fe}$, an amazing increase in the amount of Fe^{3+} cations is observed. Similar results have been obtained by Tang Ren-Yuan *et al.* (3) and F. J. Berry *et al.* (20). They found the phenomena of partial oxidation of Fe^{2+} to Fe^{3+} and of Fe_3O_4 to Fe^{3+} in the reduction processes. According to the surface interaction “incorporation model” (11), surface vacant sites exist in the surface of zirconia support, and the supported iron

TABLE 3
Mössbauer Parameters of 4 wt% $\text{Fe}_2\text{O}_3/\text{ZrO}_2$ Catalyst Treated under Various Conditions

| Treatment condition | Mössbauer parameter | | | Iron species | Relative area (%) |
|---------------------|---------------------|-------------|---------|----------------------------------|-------------------|
| | IS (mm/sec) | QS (mm/sec) | H (KOe) | | |
| As-prepared | 0.35 | 1.04 | 0 | Fe^{3+} | 100 |
| TPR to 673 K | 0.40 | 0.87 | 0 | Fe^{3+} | 55 |
| | 1.05 | 2.30 | 0 | Fe^{2+} (A) | 22 |
| | 0.28 | -0.04 | 485 | Fe^{3+} | 6 |
| | 0.66 | 0.03 | 459 | $\text{Fe}^{3+}, \text{Fe}^{2+}$ | 17 |
| TPR to 753 K | 0.40 | 0.99 | 0 | Fe^{3+} | 52 |
| | 0.99 | 0.00 | 0 | Fe^{2+} (B) | 21 |
| | 1.07 | 2.26 | 0 | Fe^{2+} (A) | 27 |
| TPR to 973 K | 0.00 | 0.00 | 340 | Fe^0 | 58 |
| | 0.37 | 1.00 | 0 | Fe^{3+} | 16 |
| | 1.15 | 2.13 | 0 | Fe^{2+} (A) | 26 |

cations can incorporate into these surface vacant sites. The interactions between iron cations and the zirconia support are very strong, and hence the reduction of these iron cations becomes very difficult. At high temperature reduction conditions, the Fe^{2+} cations which incorporate into the surface vacant sites of zirconia might migrate to the bulk phase of the zirconia support, and the solid-state reaction between zirconia and these Fe^{2+} cations could occur; hence the Fe^{2+} cations were reoxidized to Fe^{3+} cations, and the reduction of these Fe^{3+} cations became very difficult.

In summary, the pictorial models for the reduction of the 1.6 wt% $\text{Fe}_2\text{O}_3/\text{ZrO}_2$ catalyst are shown in Fig. 3.

Reduction of the High Loading (7 wt% Fe_2O_3) $\text{Fe}_2\text{O}_3/\text{ZrO}_2$ Catalyst

The room-temperature Mössbauer spectra of the as-prepared 7 wt% $\text{Fe}_2\text{O}_3/\text{ZrO}_2$ catalyst reduced at 673, 753, 973, and 1073 K, respectively, are shown in Fig. 4. The spectrum of the as-prepared sample is composed of a doublet similar to that of the 1.6 wt% $\text{Fe}_2\text{O}_3/\text{ZrO}_2$ sample and a sextet due to large particles or bulk phase $\alpha\text{-Fe}_2\text{O}_3$. The existence of the bulk phase $\alpha\text{-Fe}_2\text{O}_3$ is confirmed by the appearance of peak (b) in the TPR profile and the X-ray diffraction lines for $\alpha\text{-Fe}_2\text{O}_3$ in the XRD pattern of the sample. Upon reduction at 673 K, the bulk phase $\alpha\text{-Fe}_2\text{O}_3$ is reduced to Fe_3O_4 (Table 2). It is pertinent to note that the ratio of Mössbauer spectra are contributed by the octahedral site to that of the tetrahedral site (S) is observed to increase to a value of 3 compared to a value of 2 for the pure Fe_3O_4 , indicating there are more iron cations in B site than that for pure Fe_3O_4 . A comparison of this behavior with that noted by Lund *et al.* (4–7) and XingTao Gao *et al.* (8) in their studies on silica supported magnetite and titania supported magnetite lead to the suggestion that the iron cations in tetrahedral sites in the zirconia supported Fe_3O_4 are substituted by zirconium cations from the support, resulting in the increase in S. A weak shoulder peak at 643 K is observed in the TPR profile, indicating that some small $\alpha\text{-Fe}_2\text{O}_3$ particles are reduced to Fe^{2+} cations. But the Mössbauer parameters assigned to these Fe^{2+} cations are not obtained in the Mössbauer data, due to that the spectrum is very complex and the content of these Fe^{2+} cations is rather low.

After the sample is treated at 753 K, it is observed that the two sextets assigned to Fe_3O_4 are substituted by a singlet assigned to Fe^{2+} cations (21, 22). Moreover the amount of Fe^{3+} cations increase, indicating the partial oxidation of Fe_3O_4 to Fe^{3+} in the reduction process. It is also interesting to find that the chemical circumstance of these Fe^{2+} cations obtained by reduction of the Fe_3O_4 particles which are partly substituted by zirconium cations is different from that of the Fe^{2+} cations originated from the small

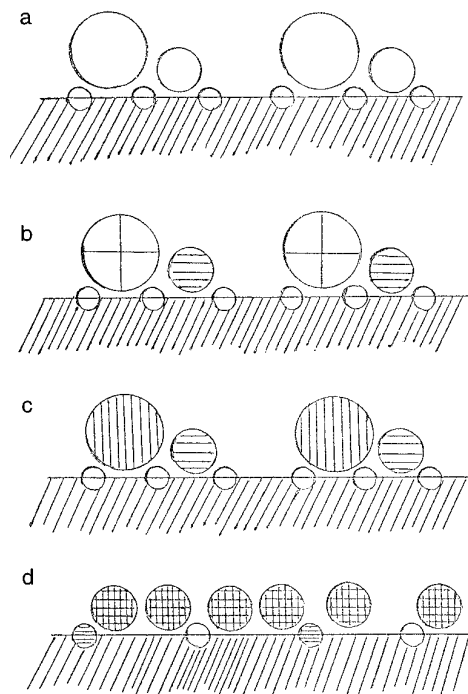


FIG. 7. Pictorial models for the reduction of the 4 wt% $\text{Fe}_2\text{O}_3/\text{ZrO}_2$ catalyst. (a) As-prepared, (b) TPR to 673 K, (c) TPR to 753 K, (d) TPR to 973 K. \circ Fe^{3+} cations from the surface iron oxides; \odot Small Fe_2O_3 particles; \ominus Bulk phase Fe_2O_3 particles; \oplus Fe^{2+} cations from the reduction of the surface Fe^{3+} cations; \otimes FeO from the reduction of the small Fe_2O_3 particles; \ominus FeO from the reduction of the Fe_3O_4 particles; \oplus Fe_3O_4 particles; \otimes Metallic iron particles; //// Surface of the zirconia support.

$\alpha\text{-Fe}_2\text{O}_3$ particles and the surface iron oxide species, as the discrepancy in their QS is very large. Further increases in the reduction temperature from 753 to 1073 K lead to more and more Fe^{3+} cations and Fe^{2+} cations reduced to $\alpha\text{-Fe}$. But some surface iron oxide species cannot be reduced due to their strong interactions with zirconia.

The pictorial models for the reduction of the 7 wt% $\text{Fe}_2\text{O}_3/\text{ZrO}_2$ catalyst are shown in Fig. 5.

Reduction of the Medium Loading (4 wt% Fe_2O_3) $\text{Fe}_2\text{O}_3/\text{ZrO}_2$ Catalyst

The room-temperature Mössbauer spectra of the as-prepared 4 wt% $\text{Fe}_2\text{O}_3/\text{ZrO}_2$ catalyst reduced at 673, 753, and 973 K, respectively, are shown in Fig. 6. For the sample with a medium iron oxide loading, peaks (a), (b), (c), and (d) can all be clearly observed in the TPR profile. We therefore assume that the large $\alpha\text{-Fe}_2\text{O}_3$ particles, small $\alpha\text{-Fe}_2\text{O}_3$ particles, and the surface iron oxide species coexist. This assumption is consistent with the results of the following Mössbauer spectroscopy (Table 3). After the sample is reduced at 673 K, three kinds of iron species are observed in the Mössbauer spectrum, namely, Fe_3O_4 originated from the reduction of the large $\alpha\text{-Fe}_2\text{O}_3$ particles, Fe^{2+} (A)

cations from the reduction of the small α -Fe₂O₃ particles, and Fe³⁺ cations from the surface iron oxide species. After an increase in the reduction temperature to 753 K, the Fe₃O₄ particles are reduced to Fe²⁺ (B) cations, and a few of the Fe³⁺ cations from the surface iron oxide species are reduced to the Fe²⁺ (A). A further increase in the reduction temperature from 753 to 973 K results in the reduction of the Fe²⁺ (B) and part of the Fe²⁺ (A) to form α -Fe, while another part of the Fe²⁺ (A) and Fe³⁺ are not reduced due to their strong interactions with zirconia.

The pictorial models for the reduction of the 4 wt% Fe₂O₃/ZrO₂ catalyst are shown in Fig. 7.

According to the above results, we can find that the reduction behavior of zirconia supported iron catalysts is quite different from that of Fe₂O₃/Al₂O₃, Fe₂O₃/SiO₂, and Fe₂O₃/TiO₂ (3–8).

CONCLUSIONS

The interactions between iron oxide and the support depend not only on the support property but also on the iron oxide loading. For the Fe₂O₃/ZrO₂ catalysts with various Fe₂O₃ loading, the dispersion states of Fe₂O₃ are quite different. The average particle size of α -Fe₂O₃ increases with increasing Fe₂O₃ loading and hence influences the interactions between Fe₂O₃ and ZrO₂. It is considered that three kinds of Fe³⁺ species exist in the sample: (i) large particles or bulk phase α -Fe₂O₃, (ii) small α -Fe₂O₃ particles, and (iii) surface iron oxide species. Reduction of the small α -Fe₂O₃ particles which have very weak interactions with zirconia is easier than that of the bulk phase α -Fe₂O₃, but the reduction of the surface iron oxide species is much

more difficult due to the strong interactions between iron oxide and zirconia.

ACKNOWLEDGMENT

The support of the National Natural Science Foundation of China is gratefully acknowledged.

REFERENCES

1. A. Baiker, R. Schlogl, E. Armbruster, and H. J. Güntherodt, *J. Catal.* **107**, 221 (1987).
2. J. Barralt and C. Renard, *Appl. Catal.* **14**, 133 (1985).
3. Tang Ren-Yuan, Zhang Su, Wang Changyu, Liang Dongbai, and Lin Liwu, *J. Catal.* **106**, 440 (1987).
4. C. R. F. Lund and J. A. Dumesic, *J. Phys. Chem.* **85**, 3175 (1981).
5. C. R. F. Lund and J. A. Dumesic, *J. Phys. Chem.* **86**, 130 (1986).
6. C. R. F. Lund and J. A. Dumesic, *J. Catal.* **72**, 21 (1981).
7. C. R. F. Lund and J. A. Dumesic, *J. Phys. Chem.* **76**, 93 (1982).
8. XingTao Gao, Jianyi Shen, and Yuanfu Hsia, *J. Chem. Soc. Faraday Trans.* **89**, 1079 (1993).
9. D. M. Rethwisch and J. A. Dumesic, *J. Phys. Chem.* **90**, 1863 (1986).
10. S. Yuen, Y. Chen, and J. E. Kubsh, *J. Phys. Chem.* **56**, 3022 (1982).
11. Yi Chen and Lifeng Zhang, *Catal. Lett.* **12**, 51 (1992).
12. T. Yoshika, J. Koezuka, and H. Ikoma, *J. Catal.* **16**, 264 (1970).
13. M. Hobson Jr. and A. D. Campbell, *J. Catal.* **8**, 294 (1967).
14. M. Hobson Jr. and H. M. Gager, *J. Catal.* **16**, 254 (1967).
15. A. Sofianos, *Catal. Today* **15**, 149 (1992).
16. F. J. Berry, S. Jobsen, and M. R. Smith, *Hyperfine Interact.* **46**, 607 (1989).
17. Jianyi Shen, Su Zhang, and Dongbai Liang, *et al.*, *J. Catal. (China)* **9**, 115 (1988).
18. A. J. H. M. Koch, H. M. Fortuin, and J. W. Geos, *J. Catal.* **96**, 261 (1985).
19. R. M. Levy and D. J. Bauer, *J. Catal.* **9**, 76 (1967).
20. F. J. Berry, Du Hongzhang, and Simon Jobson, *et al.*, *J. Chem. Soc. Chem. Commun.* 186 (1987).
21. C. A. McCammon and D. C. Price, *Phys. Chem. Miner.* **11**, 250 (1985).
22. C. A. McCammon, *J. Magn. Magn. Mater.* **104–107**, 1937 (1992).